Nonlinear theory of a laser with injected atomic coherence

J. Bergou, J. Zhang, and A. Hourri
Department of Physics, Hunter College, 695 Park Avenue, New York, New York 10021
(Received 8 July 1993; revised manuscript received 14 June 1994)

The influence of injected atomic coherence on a laser's operation is discussed by analyzing the semiclassical equations of motion of this system. Both stationary-steady-state and time-dependent regimes of operation are investigated. We present the dependence of the stationary laser intensity and phase on the external parameters (population inversion, amplitude of atomic coherence, and detuning). For small cavity-field detuning and large atomic coherence, both frequency and phase locking occurs. The laser frequency is locked to the atomic frequency, and the phase is locked to a value determined primarily by the phase of the atomic coherence. Under certain conditions, in the inverted regime, the output intensity is an S-shaped function of the atomic coherence, leading to the possibility of a bistable behavior. However, only a portion of the bistable curve gives stable stationary operation, and in critical points (the location of which depends crucially on the external parameters) time-dependent instabilities branch away. When the detuning is larger than a critical value there is neither phase nor frequency locking. We find that the time-dependent behavior of the laser intensity in this case is oscillatory (quasiperiodic), and show that there is a stable limit cycle in the phase plane of the quadratures. There is a small parameter region where a stationary steady state and an oscillatory state may coexist. We also consider the nonlinear quantum theory of a laser with injected atomic coherence, and include the effect of pumping statistics. We derive the Fokker-Planck equation for the P representation, and express the noise in terms of moments. We find that in the steady state the intensity noise can be suppressed below the shot-noise limit but that the phase fluctuations are not affected by pump regularity. For nonzero detuning, we find that transient squeezing of the phase fluctuations is possible.

PACS number(s): 42.50.Lc, 42.50.Dv, 42.60.Lh, 42.60.Mi

I. INTRODUCTION

Since the initial development of the quantum theory of the laser more than 20 years ago [1], much theoretical and experimental effort has been devoted to the problem of quantum-noise reduction in the output field. One of the earliest proposals was the laser with an injected signal [2]. In this system, the phase is not a freely diffusing quantity any longer due to phase locking to a value determined by the phase of the external signal. While this results in a reduction of the net phase fluctuation noise it leaves the fundamental sources of noise, spontaneous emission in particular, unchanged. It is not surprising therefore that, although the original idea of a laser with injected signal was directed towards stabilization of the output intensity and phase or mode selection, the system became the prime candidate for the study of instabilities (quite in line with some of the findings of the present paper) and chaos in a quantum optical system (for recent development and a review of existing work in this area, see, e.g., Ref. [3]).

A closely related idea, but one which also targets the microscopic mechanism of the emission of light, assumes preparation of the active atoms in a coherent superposition of all levels participating in the laser operation. Following the original suggestion [4], recently a considerable amount of theoretical work (semiclassical as well as quantum theory) has been directed towards lasers with injected atomic coherence [5–9]. It has been demonstrated that with a proper relation among the initial atomic coherence of randomly injected atoms, it is possible to reduce both the photon-number noise and phase noise in the laser simultaneously [5]. Furthermore, the injected atomic coherence plays the role of an injected signal in achieving phase locking [6,7] and may lead to lasing without inversion (LWI) [8]. In these latter systems LWI may be accompanied by noise quenching with a proper choice of the initial atomic coherence [9].

These features prompt us to investigate the laser with coherent initial conditions for the active atoms extensively. In particular, we focus on the role played by the various detunings (cavity field, atom field) in the dynamics.

An important difference between an ordinary, incoherently pumped laser and a laser with injected atomic coherence is the effect of phase locking [5–7]. In an ordinary laser, the phase of the electromagnetic field is not locked to a particular value but can freely diffuse over the entire angular interval of 2π. Injecting atoms with initial coherence, a phase information is introduced into the system and the laser phase will lock to a preferred value in steady state.

In addition in Ref. [5], we have developed the full nonlinear quantum theory of a laser with injected atomic coherence and demonstrated the possibility of reducing both the intensity and phase noise. However, that work has dealt with perfect resonance only, i.e., the cavity frequency, laser frequency, and the atomic transition frequency all coincide. In a closely related work, using semiclassical theory, Carty and Sargent [6] have studied the effect of injected atomic coherence on single-mode

frequency locking in a cavity. It has been assumed that the laser frequency coincides with the atomic transition frequency and the discussion has been restricted to cavity-atom detunings small enough to allow phase locking.

In the present paper, we will give a detailed study of the field dynamics of a laser with injected atomic coherence for arbitrary detuning. Also, we will consider the full quantum theory including fluctuations. First we will restrict our treatment to what essentially amounts to the semiclassical approximation. We rely on the results of our earlier work [5], which employed density operator methods [10], and derive from them the nonlinear equations of motion for intensity and phase. These equations exhibit the dependence of intensity and phase on the external parameters (population inversion, amplitude of atomic coherence, and detunings). They also give a simple physical picture of the time-dependent behavior of the system, as well as the steady-state characteristics. In our discussion we will investigate the stability of the assumption, made in Ref. [6], that the laser frequency locks to the atomic transition frequency. When the atoms are injected into the cavity in a coherent superposition, an additional feature appears in the coupling of the atoms with the cavity. Even if the laser frequency equals the atomic transition frequency, the coupling strength still depends on the cavity-field detuning. When this detuning is zero, we obtain total cavity resonance which represents the strongest coupling. As the detuning increases, the coupling strength decreases and, after a certain critical value, phase locking cannot be achieved.

Then, we focus on the reduction of noise in the laser with injected atomic coherence and regular pumping. The noise in the output of a laser field stems from the interactions with the gain and loss reservoirs. The search for new schemes that can reduce these fluctuations has become one of the most active fields in laser theory. The fluctuation in the number of active atoms (pump fluctuations) and spontaneous emission events (random emissions by the active atoms) contribute to the noise originating from the interaction with the gain reservoir. Vacuum fluctuations enter the cavity through the mirrors and contribute to the noise due to the interaction with the loss reservoir. These noise sources have been addressed in various works recently. Pump-noise suppressed laser schemes address the problem of pump fluctuations [11–13], the correlated-spontaneous-emission laser [4,5,14–15] targets spontaneous emission noise through the introduction of atomic coherence in the laser. These systems deal with the reduction of noise due to the interaction with the gain reservoir. Laser buildup from squeezed vacuum [16], in turn, targets the reduction of output fluctuations that originate from the interaction with the loss reservoir. This second line of investigations is somewhat less practical since in order to reduce output fluctuations one needs a field with reduced fluctuations to begin with.

Thus, we turn our attention to pump-noise suppressed and correlated emission laser (CEL) schemes. In particular, we are interested in combining these two effects and we will discuss the influence of the pumping statistics and the injected atomic coherence on the fluctuations of the laser radiation. If these two concepts are considered separately, the following results hold:

(1) In pump-noise reduced lasers [11,12], phase fluctuations are independent of the pumping statistics and intensity fluctuations can be significantly reduced, up to 50% below the shot-noise limit if the pumping noise is eliminated.

(2) In the one-photon laser with injected atomic coherence [5], the initial atomic coherence plays an important role in phase locking and noise reduction. It has been demonstrated there that with a proper relation among the initial atomic coherence of randomly injected atoms, it is possible to reduce both the intensity noise and phase noise in such a laser below the noise level of incoherently pumped lasers. However, no squeezing of either phase noise or intensity noise has been found in coherently pumped two-level one-photon laser.

In our analysis we combine the pumping statistics and the injected atomic coherence and develop the nonlinear quantum theory of this laser scheme. The key feature of our results is the coupling of these two factors. We find that the cavity-field detuning plays an important role in this coupling. It should be noted that the theory of a regularly pumped laser with coherent atomic initial conditions has been worked out by Benkert and Scully for the particular case of zero detuning [17]. Similar system with an injected resonant signal has been investigated in Ref. [18]. On resonance, of course, the question of stability does not arise. Even more important, there is no coupling between the intensity and phase noise and, thus, pump regularity does not affect the phase noise. Here we show that only the photon-number noise is squeezed in steady state if there is regular pumping. More important, however, we show that in some cases with finite cavity-field detuning there is a transient squeezing of phase noise.

This paper is organized as follows. In Sec. II we present the general equations of motion and discuss the steady-state operation. Section III deals with the problem of stability of the steady-state. Section IV is devoted to the study of nonstationary processes in the regimes with and without phase locking. They include initial transitions and quasiperiodic oscillations when the stationary steady state is missing overall. In Sec. V we derive a general Fokker-Planck (FP) equation for the scaled intensity n and phase ϕ in P representation with pumping terms. Numerical solutions for the steady state as well as time-dependent states are computed from moments of the distribution P. We also present limits (where a linearized treatment around steady state can be used) on initial intensity and detuning. The conclusions are then summarized and a relatively simple physical picture in terms of competing frequencies is given in Sec. VI.

II. EQUATIONS OF MOTION AND STEADY STATE

The system under consideration is the same as that of Refs. [5]–[7]: two-level atoms consisting of upper level a and lower level b and a single cavity mode. The atoms, initially prepared in a proper form of the atomic coher-

ence, are injected into the laser cavity at a rate r and allowed to interact with the laser field in the single mode. The initial density matrix for the jth atom injected at time t_j is

$$\rho^j(t_j)=\begin{bmatrix} \rho_{aa} & \bar{\rho}_{ab}e^{-i\nu t_j} \\ \bar{\rho}_{ba}e^{i\nu t_j} & \rho_{bb} \end{bmatrix}, \quad j=1,2,\ldots . \tag{2.1}$$

Here ν is the laser frequency. ρ_{aa}, ρ_{ab}, and $\bar{\rho}_{ab}=\bar{\rho}^*_{ba}$ are the same for all atoms. The Hamiltonian under the electric dipole and rotating wave approximations can be written as [5]

$$H=\hbar H_0+\hbar V=\hbar\left[\Omega a^\dagger a+\sum_{j=1}^{\infty}[H_j^{\rm at}+\theta(t-t_j)V_j]\right], \tag{2.2}$$

with

$$H_j^{\rm at}=\sum_{A=a,b}\omega_A|A^j\rangle\langle A^j| , \tag{2.3}$$

and

$$V_j=g\sigma_j^+a+ga^\dagger\sigma_j . \tag{2.4}$$

Here Ω is the frequency of the bare cavity eigenmode, $\mathbf{a}$ ($\mathbf{a}^+$) the field annihilation (creation) operator, $H_j^{\rm at}$ the free Hamiltonian of the jth atom, $\sigma^\pm$ the atomic raising and lowering operator. $\theta(t-t_j)$ is the step function. Finally, g is the atom field coupling constant.

The corresponding Fokker-Planck equation has been obtained in Ref. [5] by employing standard techniques of the quantum theory of the laser [10]. First, a master equation for the density operation of the field has been derived and then it has been converted into a FP equation in the P representation. From that Fokker-Planck equation, we can get a set of equations of motion for the mean and variance of the intensity and phase variables. It should be noted at this point that an identical set of equations for the mean values can be obtained from a completely semiclassical theory [19]. Thus, quantum effects are responsible for the fluctuations only. In this section we will focus on the semiclassical features of the system, without the quantum fluctuations (the behavior described by semiclassical theory). The genuine quantum effects will be discussed in Sec. V. In the absence of fluctuation terms, we obtain the following equations of motion for the scaled intensity, I ($\equiv$photon number), and phase, Ψ, of the field,

$$\frac{dI}{dt}=d_I \tag{2.5}$$

and

$$\frac{d\psi}{dt}=d_\psi . \tag{2.6}$$

Here the driving terms, d_I and d_Ψ, are given by the following expressions:

$$d_I=I\left\{\frac{\alpha(\rho_{aa}-\rho_{bb})}{1+I(\beta/\alpha)}-\gamma\right\}-\frac{2\sqrt{I}\,|S\bar{\rho}_{ab}|}{1+I(\beta/\alpha)}\sin(\psi-\theta+\arctan\delta) \tag{2.7}$$

and

$$d_\psi=\nu-\Omega-\frac{\alpha(\rho_{aa}-\rho_{bb})}{1+I(\beta/\alpha)}\frac{\delta}{2}-\frac{|S\bar{\rho}_{ab}|}{\sqrt{I}\,[1+(\beta/\alpha)]}\{\cos(\psi-\theta+\arctan\delta)+I(\beta/\alpha)\sqrt{1+\delta^2}\cos(\psi-\theta)\} . \tag{2.8}$$

In the above expressions we introduced the following notations: gain coefficient, $\alpha=2rg^2/(\Gamma^2+\Delta^2)$; saturation parameter, $\beta=8rg^4/(\Gamma^2+\Delta^2)^2$; field-coherence coupling, $S=rg/(\Gamma+i\Delta)$; scaled atom-field detuning, $\delta=\Delta/\Gamma$; the cavity loss rate, γ; and finally, the phase of the atomic coherence, θ. Everywhere in these expressions $\Delta=\omega_a-\omega_b-\nu=\omega-\nu$ is the atom-field detuning and Γ is the atomic decay constant (for simplicity assumed to be the same for all levels).

In steady state $d/dt=0$, the left-hand side of Eqs. (2.5) and (2.6) is zero. The laser intensity and phase are locked to their respective stationary values, I_0 and ϕ_0. The resulting equations become more transparent if we express them in terms of the scaled quantities: $n_0=I_0(\beta/\alpha)$ (photon number vs saturation parameter), $\phi_0=\Psi_0-\theta$ (phase relative to the phase of the injected coherence), $D=(\nu-\Omega)/\gamma$ (cavity-field detuning), $G=\alpha(\rho_{aa}-\rho_{bb})/\gamma-1$ (gain), $C=\alpha|\rho_{ab}|/\gamma$ (amplitude of atomic coherence). First, we want to study the stability of the states resulting from the assumption of frequency locking, $\delta=0$, which was the crucial point of Ref. [6]. Under these conditions Eqs. (2.5) and (2.6) yield for the steady state

$$G-n_0-\frac{2C}{\sqrt{n_0}}\sin\phi_0=0 \tag{2.9}$$

and

$$D-\frac{C}{\sqrt{n_0}}\cos\phi_0=0 . \tag{2.10}$$

To solve for the steady-state intensity n_0, we can eliminate the steady-state phase, ϕ_0, from the above equations, giving

$$n_0^3-2Gn_0^2+\{4D^2+G^2\}n_0-4C^2=0 . \tag{2.11}$$

This is a cubic algebraic equation for n_0. Similarly, after eliminating n_0, we can find a cubic equation for the tangent of the steady phase ϕ_0, $T=\tan\phi_0$,

$$T^3-\frac{G}{2D}T^2+T+\frac{C^2}{2D}-\frac{G}{2D}=0 . \tag{2.12}$$

Equations (2.11) and (2.12) represent the equation of state of the laser with injected atomic coherence in the

stationary steady state provided a solution exists. The equations depend on three external parameters: gain, G, coherence, C, and detuning, D. Depending on the values of the parameters, there can be one or three real solutions. In the following section we will systematically investigate these solutions from the point of view of their stability, finding those regions in the G, C, D parameter space where a single solution exists, two stable solutions may coexist, instabilities develop, etc.

In the remainder of this section we present numerical results for the state equations for two typical choices of the parameters. First, we note that in an ordinary incoherently pumped laser population inversion, $\rho_{aa}-\rho_{bb}>0$, is necessary for laser operation. However, in a laser with atomic coherence, population inversion is not necessary because the atomic coherence, $|\bar{\rho}_{ab}|$, acts as a driving force for the laser intensity. In Fig. 1 we plot the laser intensity, n_0 and phase term T, as a function of the coherence parameter, C, for three typical values of the gain G and with $D=0.25$. There is one steady-state solution for each value of C. We will find in next section that the system with negative population inversion ($G<-1$) is always stable. It is also stable in the region $-1<G<0$ where the inversion is positive but the laser is still below the resonant threshold. In the region $0<G<(12)^{1/2}D$ (gain between the resonant and off-resonant threshold) the dashed part of the curve in Fig. 1(c) becomes unstable. The phase shows an entirely similar smooth behavior as a function of C, the locking is always such that $-\pi/2<\phi_0<0$.

In the region $G>(12)^{1/2}D$ the plot of n_0 as a function of C, obtained from Eq. (2.11), becomes S shaped, indicating the emergence of a possible bistable behavior in the above threshold regime of operation. As shown in Figs. 2–4 (thin lines), there are three possibilities. Either part of the lower branch and the entire upper branch (Fig. 2), or the entire upper branch and none of the lower portions (Fig. 3), or just a part of the upper branch (Fig. 4) can be stable. Stable portions are denoted by solid line,

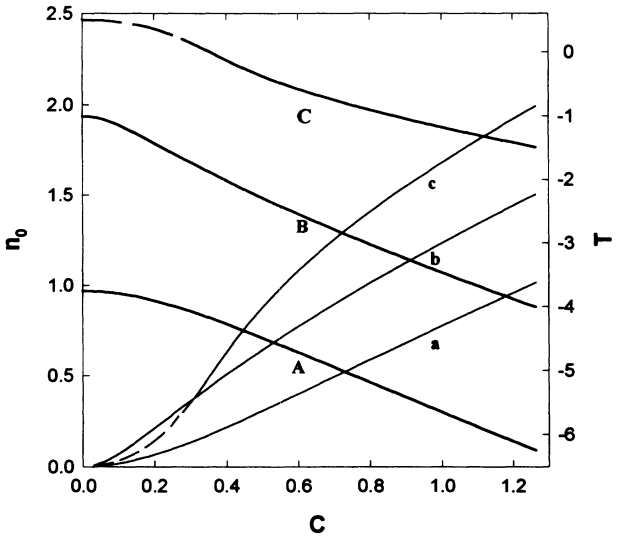

FIG. 1. Steady-state scaled intensity, n_0 (thin lines), and tangent of the steady-state phase, $T=\tan\phi_0$ (thick lines), vs the amplitude of atomic coherence, C, in the region below threshold and for (a) and (A) $D=0.2$, $G=-1.5$; (b) and (B) $D=0.25$, $G=-0.5$; (c) and (C) $D=0.5$, $G=0.5$. Solid line corresponds to stable steady state, dashed line to unstable steady state. The scale on the left-hand side (right-hand side) is for the thin lines (thick lines).

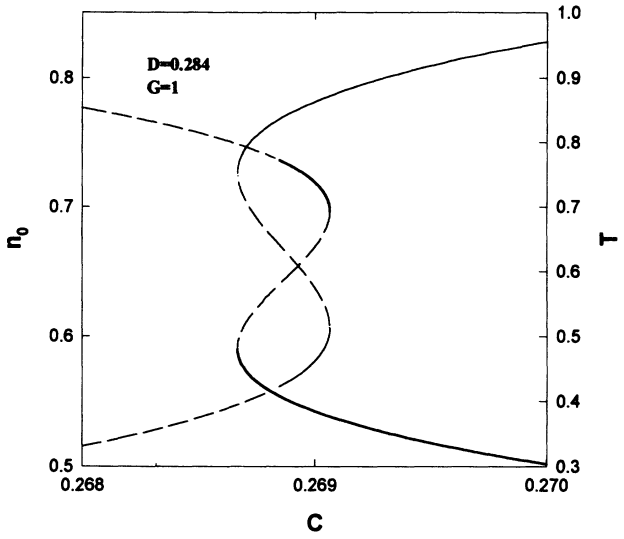

FIG. 2. Steady-state scaled intensity, n_0 (thin lines) and tangent of the steady-state phase, $T=\tan\phi_0$ (thick lines), vs C in the region above threshold and $D=0.284$, $G=1$. Solid line corresponds to stable steady state, dashed line to unstable steady state.

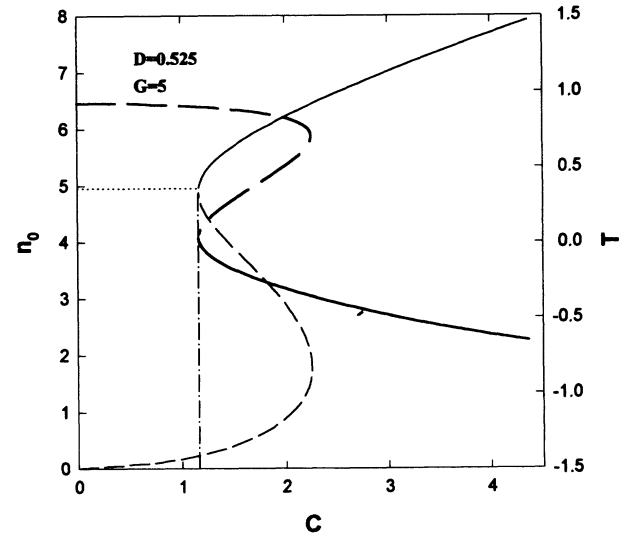

FIG. 3. Steady-state scaled intensity, n_0 (thin lines) and tangent of the steady-state phase, $T=\tan\phi_0$ (thick lines), vs C in the region above threshold and $D=0.525$, $G=5$. Solid line corresponds to stable steady state, dashed line to unstable steady state.

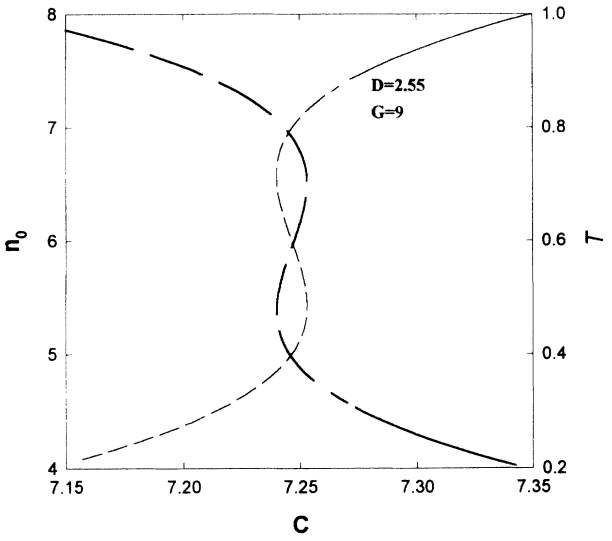

FIG. 4. Steady-state scaled intensity, n_0 (thin lines) and tangent of the steady-state phase, $T=\tan\phi_0$ (thick lines), vs C in the region above threshold and $D=2.55$, $G=9$. Solid line corresponds to stable steady state, dashed line to unstable steady state.

unstable ones by dashed line. In Figs. 2–4 we also plot T (thick lines) as a function of C. These plots, too, are again S shaped and stable and unstable parameter regions coincide with those of n_0. We note that as D increases, the gap between the vertical axis and the turning points of the S-shaped curves also increases. Since it is essentially in this gap region where most of the instabilities occur we can say that with the increase of the detuning the region of unstable behavior also increases.

Figures 1 to 4 illustrate the two basic possibilities: either monotonic dependence on the atomic coherence as in the region below ordinary laser threshold or a multivalued characteristics as in the region above the threshold.

III. STABILITY OF THE STEADY STATE

We study the stability of steady-state by employing the methods of normal mode analysis. In the neighborhood of steady-state I_0 and ϕ_0, the intensity $I(t)$ and phase $\phi(t)$ may be written as

$$I(t)=I_0+\Delta I \ ; \quad \phi(t)=\phi_0+\Delta\phi \ . \tag{3.1}$$

Substituting (3.1) into the equations of motion (2.5) and (2.6) and expanding d_I and d_ϕ around I_0 and ϕ_0 to first order in ΔI and $\Delta\phi$, neglecting higher order terms in the perturbations, we get the set of linearized equations

$$\frac{\partial\Delta I}{\partial t}=\left[\frac{\partial d_I}{\partial I}\right]_0\Delta I+\left[\frac{\partial d_I}{\partial\phi}\right]_0\Delta\phi \tag{3.2}$$

and

$$\frac{\partial\Delta\phi}{\partial t}=\left[\frac{\partial d_\phi}{\partial I}\right]_0\Delta I+\left[\frac{\partial d_\phi}{\partial\phi}\right]_0\Delta\phi \ . \tag{3.3}$$

The subscript 0 means that the derivatives have to be evaluated in the steady state. Since this is a system of linear equations we can assume that a simple exponential solution, $\Delta I(t)=\Delta I(0)e^{\lambda t}$ and $\Delta\phi(t)=\Delta\phi(0)e^{\lambda t}$, exists. Substituting this ansatz into the above equations yields the following characteristic equation for λ,

$$\lambda^2-\lambda\left[\frac{\partial d_I}{\partial I}+\frac{\partial d_\phi}{\partial\phi}\right]+\left[\frac{\partial d_I}{\partial I}\frac{\partial d_\phi}{\partial\phi}-\frac{\partial d_I}{\partial\phi}\frac{\partial d_\phi}{\partial I}\right]=0 \ . \tag{3.4}$$

For the sake of simplicity we have omitted the subscripts from the derivatives.

In view of our ansatz for the solution any initial deviation from the steady state will decay exponentially in time if $\mathrm{Re}\lambda<0$, where Re stands for the real part. Thus, this is just the condition of stability of the steady states. Applying Hurwitz's criteria, for the negative definiteness of the roots of a quadratic equation, to Eq. (3.4) gives two relations between the coefficients:

$$\frac{\partial d_I}{\partial I}\frac{\partial d_\phi}{\partial\phi}-\frac{\partial d_I}{\partial\phi}\frac{\partial d_\phi}{\partial I}>0 \tag{3.5}$$

and

$$\frac{\partial d_I}{\partial I}+\frac{\partial d_\phi}{\partial\phi}<0 \ . \tag{3.6}$$

Using the expressions for the drift coefficients, Eqs (2.7) and (2.8), and the steady-state conditions, Eqs. (2.9) and (2.10), we can easily evaluate the left-hand side of Eq. (3.5), yielding

$$4D^2+G^2-4Gn_0+3n_0^2>0 \ . \tag{3.7}$$

By comparing this expression to the equation for steady state, Eq. (2.11), we can see that it is equivalent to

$$\frac{\partial n_0}{\partial C}>0 \ . \tag{3.8}$$

This is our first condition of stability. The other condition can easily be derived from Eq. (3.6). Again, using the explicit expressions for the drift coefficients and the steady-state conditions, we obtain

$$n_0^2+(4-G)n_0-2G>0 \ . \tag{3.9}$$

This inequality is satisfied for $n_0<n_{0,1}$ and $n_0>n_{0,2}$, where $n_{0,1}$ and $n_{0,2}$ are the roots of the quadratic expression on the left-hand side, arranged in such a way that $n_{0,1}<n_{0,2}$. The explicit expressions for the roots, from Eq. (3.9), are

$$n_{0,1}=\frac{G-4-\sqrt{G^2+16}}{2} \tag{3.10}$$

and

$$n_{0,2}=\frac{G-4+\sqrt{G^2+16}}{2} \ . \tag{3.11}$$

From Eq. (3.10) $n_{0,1}<0$ always, independently of the value of G. Since $n_0>0$, by its definition, $n_{0,1}$ falls in the unphysical region and the inequality $n_0<n_{0,1}$ does not give additional condition for the stability. On the other hand, $n_{0,2}$ may fall in the physical region and the inequality $n_0>n_{0,2}$ may yield a second condition for the stability. As we shall see later, in this case the point $n_{0,2}$ is the critical point at which a Hopf bifurcation occurs. Therefore, with the notation $n_{0,2}=n_c$, the above requirement can be written as

$$n_0>n_c \ , \quad \text{where } n_c=\frac{G-4-\sqrt{G^2+16}}{2} \tag{3.12}$$

This is our second condition of stability. In the following, we shall apply the two conditions, Eqs. (3.8) and (3.12), to the investigation of the stability of the single-valued steady state (the region below ordinary laser threshold) and multivalued steady state (the region above the ordinary laser threshold) separately.

A. Stability of the single-valued steady states

When we have a single-valued steady state the first condition, Eq. (3.8), holds automatically. The slope of the intensity vs coherence curve is given by Eq. (3.7). From this equation it follows that the steady state is single valued (the slope does not change sign) if $G\leq(12)^{1/2}D$ and multivalued otherwise [see Eqs. (3.13) and (3.14) below]. We can now distinguish between the regions $G<0$ and $0\leq G\leq(12)^{1/2}D$. It should be noted at this point that $G_{\text{th},1}=0$ is the threshold for the corresponding incoherently pumped laser without detuning and the expression $G_{\text{th},2}=(12)^{1/2}D$ is the laser threshold for the corresponding incoherently pumped laser with detuning.

(i) In the region $G<0$ (or, equivalently, $G<G_{\text{th},1}$) the critical point, n_c, defined in Eq. (3.13), is negative and the second stability condition, given in the same equation, is satisfied for all $n_0>0$, i.e., in the entire physical region. No part of the curves (a) and (b) in Fig. 1 becomes unstable, for any value of the external control parameters.

(ii) In the region $0\leq G\leq(12)^{1/2}D$ (or, equivalently, $G_{\text{th},1}\leq G\leq G_{\text{th}.2}$) the photon number n_0 continues to be a single-valued function of the coherence parameter C. In this region, however, $n_c>0$. Applying the second stability condition, Eq. (3.12), to this case gives that the part of the curve (c) in Fig. 1, where $0\leq n_0<n_c$, is unstable (denoted with dashed line). Here n_c is a Hopf bifurcation point and in the region between the origin and n_c periodic oscillations occur. They branch away continuously from the steady-state curve which, thus, is stable above the critical point. The region below the critical point, where the oscillations take place, will be studied in Sec. IV.

Summarizing the findings of this subsection we can conclude that the steady state is single valued if $G\leq G_{\text{th},2}$. The entire steady-state curve is stable if $G\leq G_{\text{th},1}$ and the section between the origin and the critical point is unstable if $G_{\text{th},1}<G\leq G_{\text{th},2}$. Entirely similar conclusion hold for the phase plots in Fig. 1 (thick lines).

B. Stability of the multivalued steady states

When we are dealing with a multivalued steady state, i.e., the plot of the photon number vs coherence is S shaped as in Figs. 2–4 (thin lines) then the first stability condition, Eq. (3.8), tells us that the portion with negative slope (the middle section of the S) is unstable. To investigate this case further we note that the two turning points of the S-shaped curve can be calculated from the zeros of the left-hand side of Eq. (3.7) since in these points the slope of the curve changes its sign. The turning points are then given by

$$n_1=\frac{2G-\sqrt{G^2-12D^2}}{3} \tag{3.13}$$

and

$$n_2=\frac{2G+\sqrt{G^2-12D^2}}{3} \ , \tag{3.14}$$

so that $n_1<n_2$. Obviously, we need $G>G_{\text{th},2}$ to have two real turning points or a multivalued steady state. Conversely, in the region $G\leq G_{\text{th},2}$ the steady state is single valued, a condition that we used in connection with the stability analysis in Sec. III A. It should be noted that, since $G>0$, n_c is always positive and, thus, a part of the S-shaped function is always unstable. We can now distinguish three different parameter regions: I $n_c<n_1$, II $n_1\leq n_c\leq n_2$, and III $n_2<n_c$. In region I the part of the curve with $n_0<n_c$ on the lower branch in Fig. 2 is unstable. The rest of the lower branch and the entire upper branch are stable. Between the stable parts of the upper and lower branches steady-state bistable behavior is expected. Beyond the Hopf bifurcation point, n_c, located on the lower branch periodic oscillations appear. In region II, n_c falls on the globally unstable middle branch

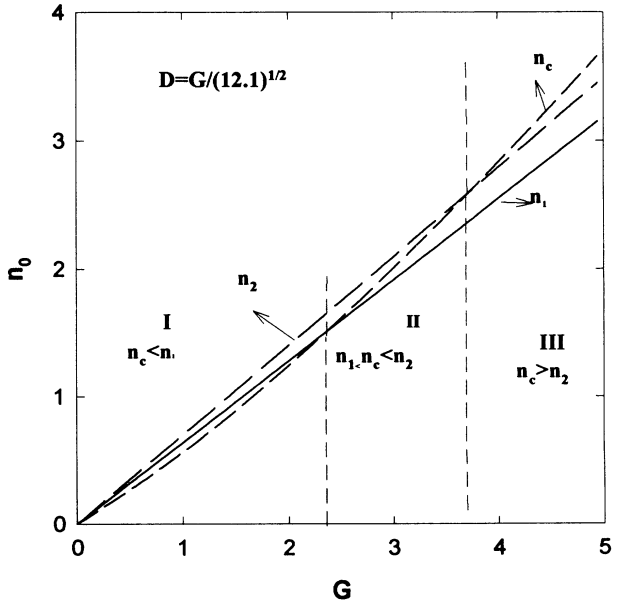

FIG. 5. The critical point, n_c, and the lower and upper turning points, n_1 and n_2, vs G for $D=G/\sqrt{12.1}$.

and is never realized. In this case, the upper turning point becomes an effective critical point beyond which non-Hopf oscillations appear. The entire upper branch is stable. This situation is depicted in Fig. 3. Finally, in region III the critical point is located on the upper branch. Beyond the critical point stable periodic oscillations evolve. The rest of the upper branch, $n_0 > n_c$, is stable. A typical situation is shown in Fig. 4. It should be mentioned at this point that the phase diagrams, thick lines, exhibit a very similar behavior. In particular, stable regions, turning points, and the critical point all occur at the same parameter values.

In Figs. 5–7 we summarize these findings. In Fig. 5 the turning points, n_1, n_2, and the critical point, n_c, are depicted as functions of the gain parameter, G, for $D^2=G^2/12.1$. The regions correspond to the regions discussed above. In region I part of the lower branch is unstable, the critical point is a Hopf bifurcation point. In region II the entire upper branch is stable, the upper turning point is the effective non-Hopf bifurcation point. In region III part of the upper branch is stable, the critical point is again a Hopf bifurcation point. In Fig. 6 we display the G-D parameter plane. In this plane the equations $G=(12)^{1/2}D$, $n_c=n_1$, and $n_c=n_2$ correspond to lines and play the role of separatrixes. They separate the parameter plane into five regions. Above the line $G=(12)^{1/2}D$ is region A (ii) of the previous subsection, where n_0 is a single-valued function of C, as in Fig. 1(c), since $0<G^2<12D^2$. The region below this line is region B investigated in this subsection. The other two lines divide region B further. In region I, some part of the lower branch and the entire upper branch are stable. In region II, only the upper branch is stable and the upper turning point is a non-Hopf bifurcation point. Finally, in region III, only part of the upper branch is stable. In Fig. 7 we display the D-C parameter plane as for Fig. 6. Region I is so small in this plane that we show the lower left corner of Fig. 7, region I, enlarged in the inset in order to make it visible.

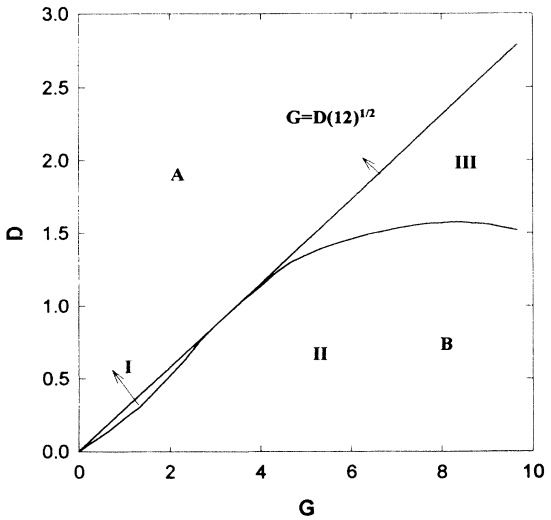

FIG. 6. Projection of the D, G, C parameter space onto the D-G plane. The different regions correspond to the different stability regions discussed in the text.

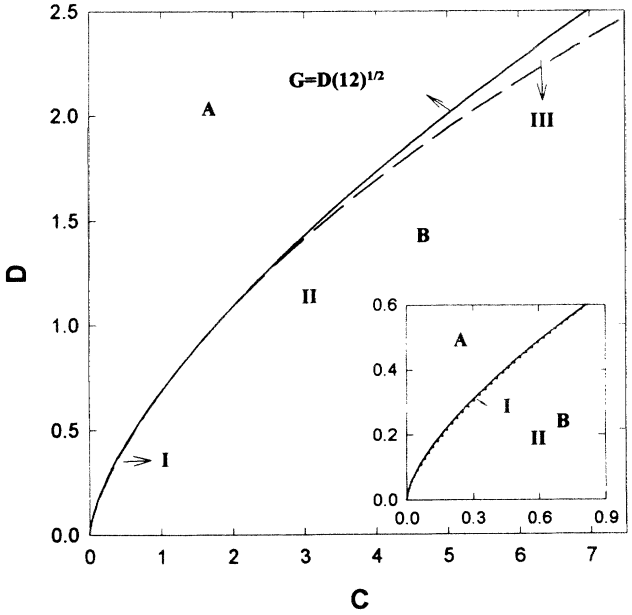

FIG. 7. Projection of the D, G, C parameter space onto the C-D plane. The inset shows the lower left corner of the main plot enlarged to exhibit region I more clearly.

IV. DYNAMICAL EVOLUTION

So far, we have dealt with the steady states of the system by replacing the time derivatives with zero on the left-hand side of Eqs. (2.5) and (2.6). Let us now consider time-dependent scenarios by keeping the full time dependence in the equations. In this section we shall investigate time evolution from a given initial condition. In particular, in Part A we shall study how the system approaches steady state in those regions of the external control parameters where they exist. In Part B we shall investigate the states that evolve from a given initial state in the unstable regions.

First, we rewrite Eqs. (2.5) and (3.6) in terms of the scaled external parameters introduced in Eqs. (2.7) and (2.8) and the scaled photon number and phase, n and ϕ, which are obvious generalizations of n_0 and ϕ_0 for the time dependent case, as

$$\frac{dn}{d\tau}=d_n \ , \tag{4.1}$$

with

$$d_n=n\frac{G-n}{1+n}-\frac{2\sqrt{nC}}{1+n}\sin\phi \ , \tag{4.2}$$

and

$$\frac{d\phi}{d\tau}=d_\phi \ , \tag{4.3}$$

with

$$d_\phi = D - \frac{C}{\sqrt{n}} \cos\phi \ . \tag{4.4}$$

In these equations we introduced the scaled time variable, $\bar{t} = \gamma t$. The nonlinear dynamics of the system is completely determined by Eqs. (4.1)–(4.4).

A. Transients around stable steady states

The above equations allow for an approximate separation of the dynamics of the phase and intensity in the vicinity of the critical point, n_c. Equations (4.1) and (4.2) then determine the intensity and Eqs. (4.3) and (4.4), being just the phase-locking equation, the phase. Further away from n_c, the dynamics of the phase and intensity become entangled. Instead of separately giving the results of the analytical treatment for the neighborhood of the critical region we just present the numerical results, valid for a broad range of parameters.

We can get some analytical insight into the relaxation dynamics by studying the trajectories in the n-ϕ plane. By transforming Eqs. (4.1) and (4.3) to the form

$$\frac{dn}{d\phi} = \frac{d_n}{d_\phi} \ , \tag{4.5}$$

we can obtain the governing equation. Since the time $\bar{t}$ does not appear explicitly in this equation, we can exhibit the integral curves in the n-ϕ plane. Each point (n,ϕ) in this plane represents a possible set of initial conditions. A trajectory going through this particular point then determines the time evolution of the system, starting from this initial condition. In Figs. 8–11 we plot the intensity n vs phase ϕ. The steady state now correspond to attractive singular points. In Fig. 9, points a and b correspond to stable upper branch and stable lower branch, respectively. In Fig. 10, corresponding to the situation

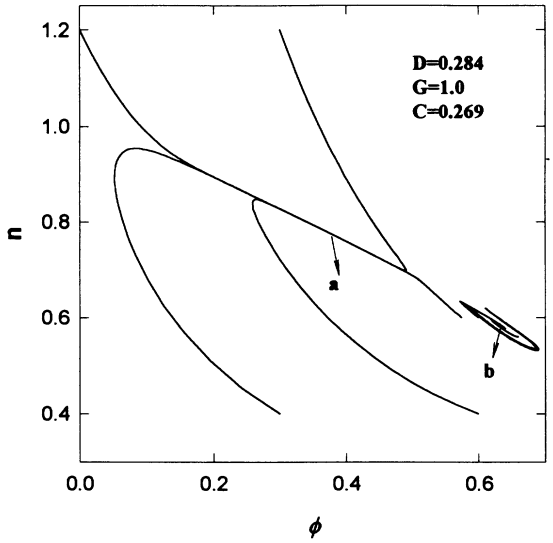

FIG. 9. n-ϕ trajectories for $C=0.269$, $D=0.284$, $G=1$ (cf. Fig. 2).

when the upper turning point is the effective critical point, there are three singularities. Point a (6.2, $-\pi/2$) is an attractive fix point (stable node, all trajectories run towards this point) and the corresponding steady state is realized. This point corresponds to the stable steady state on the upper branch in Fig. 3. Point b (3.4, $\pi/2$) is a repulsive fix point, all trajectories run away from this point. It corresponds to the unstable steady state on the middle branch. Finally, point c (0.4, $\pi/2$) is a metastable

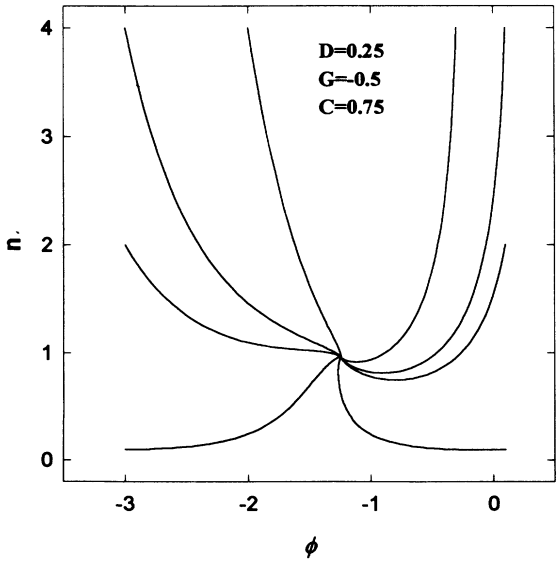

FIG. 8. n-ϕ trajectories of $C=0.75$, $D=0.25$, $G=-0.5$ [cf. line (b) in Fig. 1].

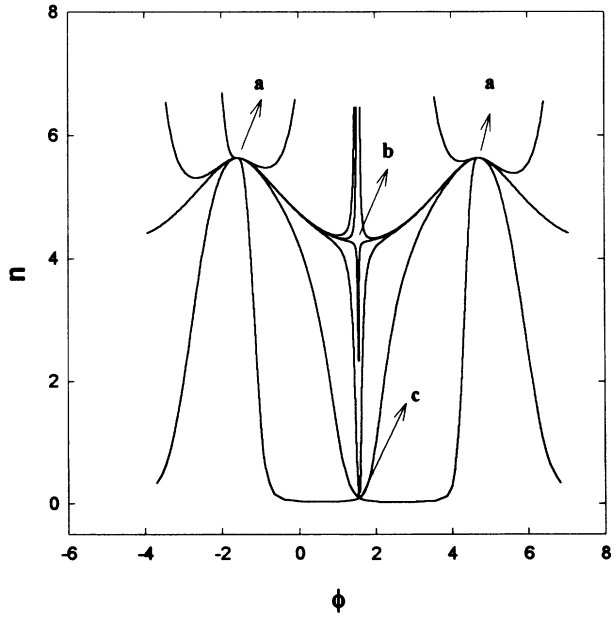

FIG. 10. n-ϕ trajectories for $C=0.75$, $D=0.525$,$G=5$ (cf. Fig. 3).

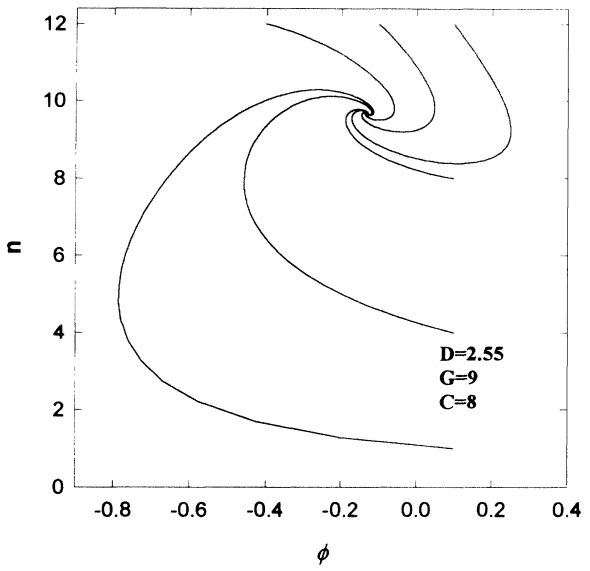

FIG. 11. n-ϕ trajectories for $C=8$, $D=2.55$, $G=9$ (cf. Fig. 4).

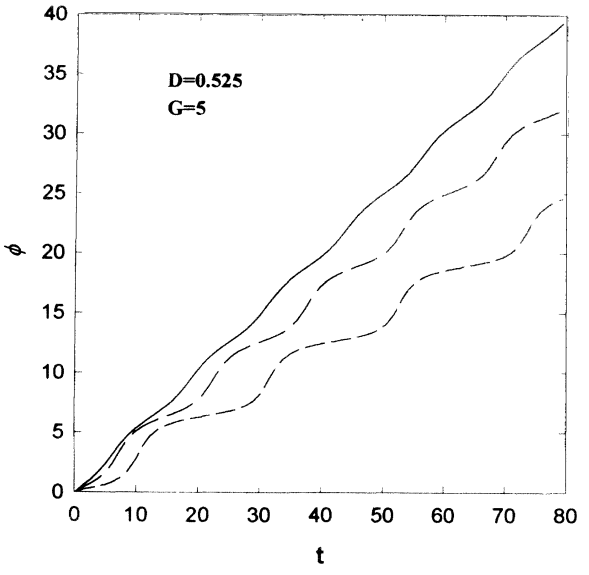

FIG. 12. Time evolution of the phase ϕ with $D=0.525$, $G=5$, $C=0.75$.

fix point with some trajectories running into others originating from it. It corresponds to the unstable steady state on the lower branch. Any slight deviation from point b or point c will result in passage to the stable point a.

In the n-ϕ plane, the point $(n(\bar{t}),\phi(\bar{t}))$ moves, with the increase of the time $\bar{t}$, along the integral curve and converges ultimately to the table point a. Thus the time-varying solutions are correlated with the trajectories of (4.5) and the steady state with the singular points, a, b, and c, in the n-ϕ plane.

B. Time evolution in the unstable regions

In this subsection, we shall discuss time evolution from a given initial condition in those regions of the external control parameters where the steady state becomes unstable, i.e., beyond the critical point. This corresponds to a choice of the initial condition such that $n(0)<n_c$. We find that $n(\bar{t})$ oscillates around a value which is very close to the critical intensity, n_c, after the initial transients have decayed. The period of oscillations, T, can be found from

$$T=\int_0^{2\pi}\frac{d\phi}{D-\frac{C}{\sqrt{n_c}}\cos\phi}=\frac{2\pi}{\left[D^2-\frac{C^2}{n_c}\right]^{1/2}}\ . \qquad (4.6)$$

The phase $\phi(\bar{t})$ vs $\bar{t}$ is depicted in Fig. 12 with $D=0.525$, $G=5$, and $C=0.75$. The time dependence has two ingredients. First, there is a constant shift of the operating frequency which results in a steady increase of the phase, strictly proportional with time. This is represented by the average slope of the phase vs time curve. Second, superimposed on this straight line development, there is a small oscillation very similar to the oscillation of the average intensity. In particular, the frequency of these phase oscillations is the same as that of the intensity oscillations, given by Eq. (4.6).

Before we develop an analytical theory of the frequency shift (the slope of the curves in Fig. 11) we display this oscillatory behavior from another point of view. Namely, we again discuss the integral curves, resulting from Eq. (4.5). This time, however, instead of displaying the trajectories in the n-ϕ plane, we will plot them in the X-Y phase plane of quadratures [20], where $X=\sqrt{n_0}\cos\phi_0$ and $Y=\sqrt{n_0}\sin\phi_0$ are the usual quadratures component variables. Figure 13 shows the trajectories in the X-Y plane with $C=0.75$ and $G=5$ and $D=0.525$. Each tra-

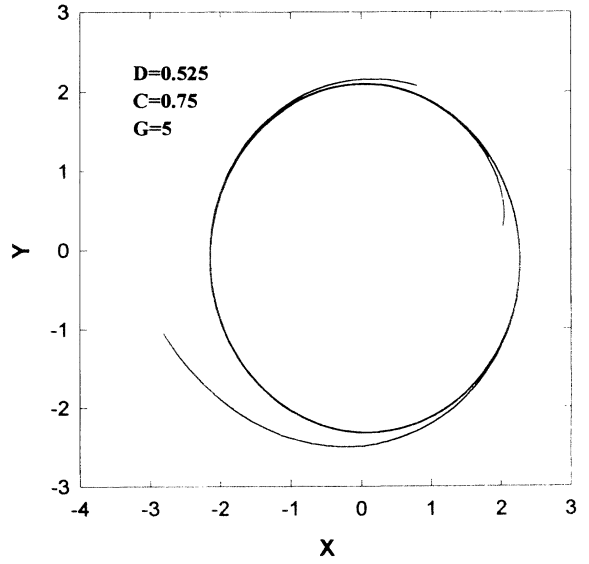

FIG. 13. Integral curves in the phase plane of quadratures, X and Y, with $D=0.525$, $C=0.75$, $G=5$.

jectory approaches a stable limit cycle. The point $(X(\bar{t}), Y(\bar{t}))$, starting from any initial condition, after the initial transients, i.e., after the approach to the limit cycle, moves along the limit cycle as $\bar{t}$ increases. The period required for the point to complete one cycle is given by (4.6).

Finally, we turn our attention to the study of the operating frequency of the laser. In our assumption, the atom-field detuning is much smaller than the cavity-field detuning, i.e., $\omega-\nu \ll \Omega-\nu$. In fact, for the case of stable frequency locking, the atom-field detuning vanishes. For the general case, we can write the field as [6]

$$E \propto e^{i\nu t} \propto e^{i\omega t-\phi} . \tag{4.7}$$

Clearly, for frequency locking $\nu=\omega$ and $\phi=$const. In the unstable regimes the phase ϕ of the electric field, in accordance with Fig. 12, can be represented as $\phi=\Delta\nu t+\Delta\phi(0)\cos(2\pi t/T)$. The deviation from the atomic frequency is given by $\Delta\nu=\langle d\phi/dt\rangle$, where $\langle\ \rangle$ stands for time average (it should be noted that frequencies are measured in units of γ and time in units of γ^{-1} throughout this section). We can now expand the general phase equation (2.6) to lowest order in γ/Γ, keeping the atomic detuning δ in it as in Eq. (2.8), around the mean values of the oscillations, $n_{\rm av}$ and $\Delta\nu t$, to obtain

$$\frac{d\phi}{d\bar{t}}=\frac{d-\dfrac{C}{\sqrt{n_{\rm av}}}\cos\phi}{1+\dfrac{G+1}{n_{\rm av}+1}\dfrac{\gamma}{2\Gamma}-\dfrac{C}{\sqrt{n_{\rm av}}}\dfrac{\gamma}{\Gamma}\sin\phi} . \tag{4.8}$$

The above expression has some interesting consequences:

(1) For $C=0$ we have

$$\frac{d\phi}{d\bar{t}}=\Delta\nu=\frac{D}{1+\dfrac{G+1}{n_{\rm av}+1}}\frac{\gamma}{2\Gamma} ,$$

giving $\nu=\omega-\Delta\nu=(2\Gamma\Omega+\gamma\omega)/(2\Gamma+\gamma)$, which is just the operating frequency of a usual incoherently pumped laser as given by the frequency pulling expression [1].

(2) If $C>C_c$ $(D<D_c)$ the phase is locked, $d\phi/dt=0$. This also involves the laser frequency being locked to the atomic frequency, $\nu=\omega$. (Here C_c and D_c are the values of the coherence and detuning, respectively, in the critical point.)

(3) For the intermediate case, when $C<C_c$ and $D>D_c$, there is no stable frequency locking. As it has already been discussed in connection with Fig. 11 the frequency is shifted from the atomic frequency and superimposed on this shift, there is also a small oscillatory part of the phase. The frequency shift is a function of the external control parameters and can be obtained in analytical form by taking the average of Eq. (4.8), yielding

$$\Delta\nu=\left\langle\frac{d\phi}{d\bar{t}}\right\rangle=\frac{\left[D^2-\dfrac{C^2}{n_{\rm av}}\right]^{1/2}}{1+\dfrac{G+1}{1+n_{\rm av}}\dfrac{\gamma}{2\Gamma}} . \tag{4.9}$$

As the amplitude of atomic coherence C increases, the average deviation decreases. When C is larger than a critical value, the average deviation is zero, i.e., frequency locking occurs. The mean operating frequency, ν, vs the coherence parameter, C, is plotted in Fig. 14 for the unstable region of operation. The result of this calculation is in excellent agreement with the average slope of the various $\phi(t)$ plots in Fig. 12.

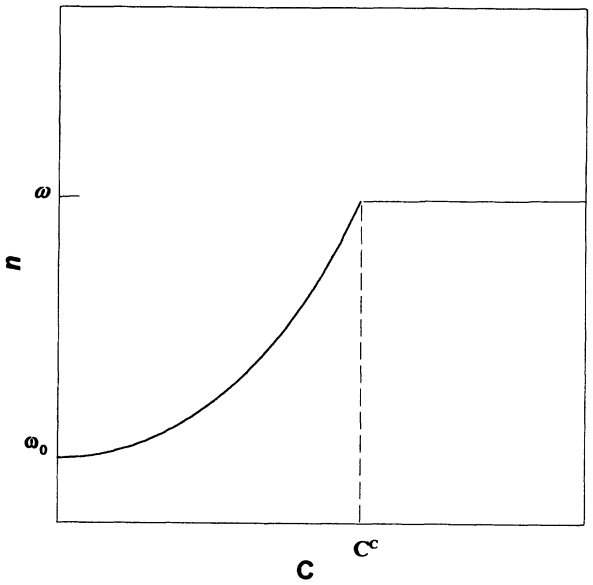

FIG. 14. Average operating frequency of the laser in the unstable region of operation. Corresponds to the average slope of the curve in Fig. 12.

V. NOISE DYNAMICS AROUND STEADY STATE

In order to consider the effect of both atomic coherence and pumping statistics on the quantum noise of the laser we adopt the following model. We assume that a beam of three-level atoms first passes through a preparation region then enters the laser cavity. In the preparation region, each atom is excited from a distant ground level c to the upper level a of the lasing transition with a probability p, and then interacts with a preparation field producing the initial atomic coherence between the upper level a and lower level b of the transition. When the atoms leave the preparation region, they have a proper form of the initial atomic coherence and pumping statistics distribution, which, in some cases, can be adequately described by the Bernoulli's distribution.

Inside the cavity, the system we are going to consider is the same as in the previous sections, except for the inclusion of pumping statistics of the atoms: two-level active atoms consisting of an upper level a and a lower level b. These active atoms are injected into the laser cavity at a rate r to interact with the laser field, and the initial density matrix is given by Eq. (2.1).

If we assume that the interaction time of each atom with the field inside the cavity is much smaller than the cavity damping time, the dissipation during the interaction can be neglected. Let the jth atom enter the cavity

at the time t_j and spend a time τ inside the cavity. We can write

$$\rho(t_j+\tau)=M(\tau)\rho(t_j) . \tag{5.1}$$

Here the operator $M(\tau)$ describes the change of $\rho(t_j)$ due to the interaction with a single atom and its explicit form will depend on the particular model under consideration.

If n atoms cross the cavity from initial time 0 to the time t, the density matrix of the field at time t is

$$\rho^{(n)}(t)=M^n\rho(0) . \tag{5.2}$$

We have taken into account the fact that each atom finds the field in the state prepared by the preceding atom.

Because the atoms have a pumping statistics distribution we must average Eq. (2.3) with the distribution. Finally, we have [11]

$$\frac{d}{dt}\rho(t)=\frac{r}{p}\ln[1+p(M-1)]\rho(t) . \tag{5.3}$$

If $M-1$ is small, we consider p an expansion parameter, and expand Eq. (5.3)

$$\frac{d}{dt}\rho(t)=r\left[(M-1)-\frac{p}{2}(M-1)^2+\cdots\right]\rho(t) . \tag{5.4}$$

In Ref. [21], we have shown that even after including the loss into the master equation, Eq. (5.4) remains valid in the sense of an asymptotic expansion to adequately describe the time rate of change of the density operator due to interactions with the gain reservoir.

In our model, we will consider a laser with the initial atomic coherence and pumping statistics, so M is the operator with the initial atomic coherence [5]. Using P representation, Eq. (5.3) can be transformed into a Fokker-Planck equation. In this paper, we want to discuss the properties of the intensity and phase of laser field. So we will express the Fokker-Planck equation in terms of intensity I and phase ψ. Introducing $n=(\beta/\alpha)I$ and $\phi=\psi-\theta$, where θ is the phase of ρ_{ab}. We have

$$\frac{\partial P}{\partial\bar{t}}=\left\{-\frac{\partial}{\partial n}d_n-\frac{\partial}{\partial\phi}d_\phi+\varepsilon\frac{\partial^2}{\partial n^2}D_{nn}+\varepsilon\frac{\partial^2}{\partial\phi^2}D_{\phi\phi}+2\varepsilon\frac{\partial^2}{\partial n\partial\phi}D_{n\phi}\right\}P , \tag{5.5}$$

$$d_n=\frac{(G-n)n}{1+n}-\frac{2\sqrt{nC}}{1+n}\sin\phi , \tag{5.6}$$

$$d_\phi=D-\frac{C}{\sqrt{n}}\cos\phi , \tag{5.7}$$

$$D_{nn}=\frac{n}{(1+n)^2}\left[\frac{A+G+1}{2}+\frac{(A-G-1)n}{2}+2C\sqrt{n}\sin\phi\right]-\frac{p}{2}n\left[\frac{n(1+G)^2}{2(1+n)^2}+\frac{2C^2\sin^2\phi}{(1+n)^2}-\frac{2(G+1)C\sin\phi\sqrt{n}}{(1+n)^2}\right] , \tag{5.8}$$

$$D_{\phi\phi}=\frac{1}{4n(1+n)}\left[\frac{A+G+1}{2}+\frac{An}{2}+C\sqrt{n}\sin\phi\right]-\frac{p}{2}\left[\frac{D^2}{2}+\frac{C^2\cos^2\phi}{2n}-\frac{D\sqrt{n}C\cos\phi}{n}\right] , \tag{5.9}$$

$$D_{n\phi}=\frac{\sqrt{n}C\cos\phi}{4(1+n)}-\frac{p}{8(1+n)}[Dn(G+1)-2D\sqrt{n}C\sin\phi-\sqrt{n}(G+1)C\cos\phi+C^2\sin2\phi] , \tag{5.10}$$

where $\varepsilon=\beta/\alpha$ and $A=\alpha/\gamma$. Here we assume the atom-field detuning to be zero.

From the Fokker-Planck equation, we can get an infinite set of ordinary differential equations for moments. If we assume the noise to be very weak, $\varepsilon\ll1$, we can truncate these equations into a finite set of nonlinear equations. In this paper, we assume that only the first- and second-order moments are nonzero. These nonzero moments obey the following equations:

$$\frac{d}{d\bar{t}}\langle n\rangle=\langle d_n\rangle , \tag{5.11}$$

$$\frac{d}{d\bar{t}}\langle\phi\rangle=\langle d_\phi\rangle , \tag{5.12}$$

$$\frac{d}{d\bar{t}}\langle(\delta n)^2\rangle=2\langle d_n\delta n\rangle+2\varepsilon\langle D_{nn}\rangle , \tag{5.13}$$

$$\frac{d}{d\bar{t}}\langle(\delta\phi)^2\rangle=2\langle d_\phi\delta\phi\rangle+2\varepsilon\langle D_{\phi\phi}\rangle , \tag{5.14}$$

$$\frac{d}{d\bar{t}}\langle(\delta n)(\delta\phi)\rangle=\langle d_n\delta\phi\rangle+\langle d_\phi\delta n\rangle+2\varepsilon\langle D_{n\phi}\rangle . \tag{5.15}$$

Here we introduced the notations $\delta n=n-\langle n\rangle$, $\delta\phi=\phi-\langle\phi\rangle$. In this section we will use these equations to discuss the steady-state noise and the dynamical noise.

A. Steady state

First, we pay attention to the steady-state diffusion coefficients. In steady state (n_0,ϕ_0), for the stable values, the value of $\sin\phi_0$ is less than zero. So both the atomic coherence ρ_{ab} and pumping statistics p can reduce the intensity diffusion coefficient D_{nn}, but only the atomic coherence C can reduce the phase diffusion coefficient $D_{\phi\phi}$. In steady state the diffusion coefficients are

$$D_{nn}^0=\frac{n_0}{(1+n_0)^2}\left[\frac{A+G+1}{2}+\frac{A-G-1}{2}n_0 +2C\sqrt{n_0}\sin\phi_0\right] -\frac{p}{2}n_0\left[\frac{n_0(1+G)^2}{2(1+n_0)^2}+\frac{2C^2\sin^2\phi_0}{(1+n_0)^2} -\frac{2(G+1)C\sin\phi_0\sqrt{n_0}}{(1+n_0)^2}\right], \tag{5.16}$$

$$D_{\phi\phi}^0=\frac{1}{4n_0(1+n_0)}\left[\frac{A+G+1}{2}+\frac{An_0}{2}+C\sqrt{n_0}\sin\phi_0\right], \tag{5.17}$$

$$D_{n\phi}^0=\frac{Dn_0}{4(1+n_0)}\ . \tag{5.18}$$

In the following we discuss the steady-state variances of the intensity and phase. In the P representation, the intensity variance is [20]

$$\langle(\Delta I)^2\rangle=\langle(\delta I)^2\rangle+\langle I\rangle\ , \tag{5.19}$$

and the phase variance is

$$\langle(\Delta\phi)^2\rangle=\langle(\delta\phi)^2\rangle+\frac{1}{4\langle I\rangle}\ , \tag{5.20}$$

where $(\delta\cdots)$ corresponds to the normal ordered part of $(\Delta\cdots)$.

Expanding d_n, d_ϕ, D_{nn}, $D_{n\phi}$, and $D_{\phi\phi}$ around steady state n_0, ϕ_0 up to the first order in δn and $\delta\phi$, we get

$$\frac{d}{dt}\langle(\delta n)^2\rangle=2\left[\frac{d}{dn}d_n\right]_0\langle(\delta n)^2\rangle +2\left[\frac{d}{d\phi}d_n\right]_0\langle(\delta n\delta\phi)\rangle+2\varepsilon(D_{nn})_0\ , \tag{5.21}$$

$$\frac{d}{dt}\langle(\delta\phi)^2\rangle=2\left[\frac{d}{d\phi}d_\phi\right]_0\langle(\delta\phi)^2\rangle +2\left[\frac{d}{dn}d_\phi\right]_0\langle(\delta n\delta\phi)\rangle+2\varepsilon(D_{\phi\phi})_0\ , \tag{5.22}$$

$$\frac{d}{dt}\langle(\delta n\delta\phi)\rangle=\left[\frac{d}{dn}d_\phi\right]_0\langle(\delta n)^2\rangle+\left[\frac{d}{d\phi}d_n\right]_0\langle(\delta\phi)^2\rangle +\left[\left[\frac{d}{dn}d_n\right]_0+\left[\frac{d}{d\phi}d_\phi\right]_0\right]\langle(\delta n\delta\phi)\rangle +2\varepsilon(D_{n\phi})_0\ . \tag{5.23}$$

By setting $d/dt=0$ in Eqs. (5.21), (5.22), (5.23), and solving for $(\delta n)^2$ and $(\delta\phi)^2$, then inserting these into (5.19) and (5.20), we can get

$$\frac{\langle(\Delta I)^2\rangle}{I}=1+\frac{D_2(D_2D_{22}-D_4D_{11}n^2-2D_3D_{12}n)+D_3n^2(D_1+D_3)D_{11}}{n^2(D_1+D_3)(D_2D_4-D_1D_3)} \tag{5.24}$$

and

$$\langle(\Delta\phi)^2\rangle I=\tfrac{1}{4}+\frac{D_4(D_4D_{11}n^2-D_2D_{22}-2D_1D_{12}n)+D_1(D_1+D_3)D_{22}}{(D_1+D_3)(D_3D_4-D_1D_3)}\ . \tag{5.25}$$

Here we introduced the notation $D_1=\partial d_n/\partial n$, $D_2=\partial d_n/\partial\phi$, $D_3=\partial d_\phi/\partial\phi$, $D_4=\partial d_\phi/\partial n$, and $D_{11}=(D_{nn})_0$, $D_{12}=(D_{n\phi})_0$, $D_{22}=(D_{\phi\phi})_0$.

Using Eqs. (5.24) and (5.25), we can plot the values of $\langle(\Delta I)^2\rangle/I$ and $\langle(\Delta\phi)^2\rangle I$ as a function of the injected atomic coherence C for several sets of parameters. Intensity noise as a function of C, for zero detuning, is plotted in Fig. 15. The dashed line is for random pumping ($p=0$), solid line for regular pumping ($p=1$). The parameters are $D=0$, $G=5$, and $A=7.5$. Phase noise is shown in Fig. 16 and parameters are the same as in Fig. 15. We find that the injected atomic coherence can reduce both the intensity and phase noise and the larger the injected atomic coherence, the lower the noise. Also we find that pump regularity is a very important factor for intensity noise squeezing but has no effect on the phase noise under the condition of zero detuning. In Fig. 15 there is almost 75% squeezing in the laser intensity for $C=2.25$. We notice that the range of ρ_{ab} depends on ρ_{aa} and ρ_{bb}, that is $0\le\rho_{ab}\le(\rho_{aa}\rho_{bb})^{1/2}$. For our parameters, the range of ρ_{ab} is $0\le\rho_{ab}\le0.3$, so the range of C is $0\le C\le2.25$.

In Figs. 17 and 18 we plot the intensity noise and phase noise, respectively, as a function of detuning D, with $A=2.5$, $G=-1$, and $C=1.25$.

Though the noise with detuning is still larger than the noise without detuning for the same initial atomic coherence C, the coupling of initial atomic coherence C and

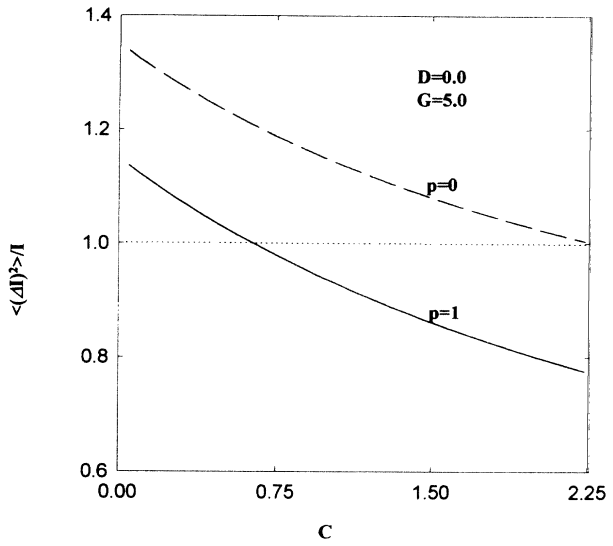

FIG. 15. Intensity noise as a function of the amplitude of atomic coherence C with $A=7.5$, $D=0$, and $G=5$ for $p=0$ (dashed line) and $p=1$ (solid line). The dotted line corresponds to the vacuum noise level.

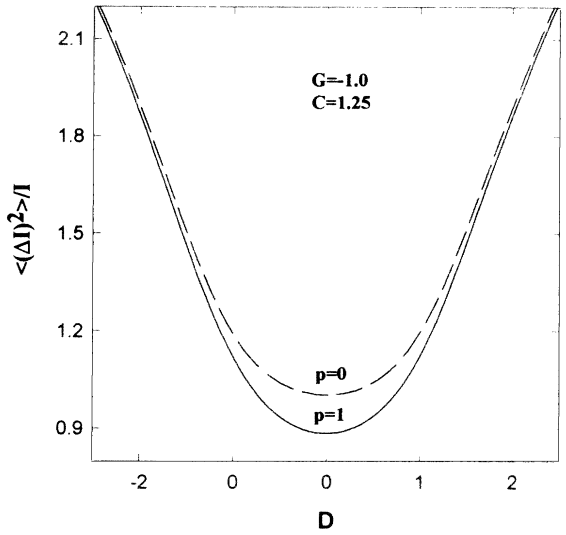

FIG. 17. Intensity noise as a function of detuning D with $A=2.5$, $G=-1$, and $C=1.25$.

pumping statistics p suggest a way to reduce or even squeeze the noise of the laser field. We will discuss this aspect later.

B. Time-dependent behavior

In the previous sections we investigated both steady state and time-dependent regimes of operation. Here we will study the transient behavior of the noise around both stationary steady states and time-dependent mean values.

Expanding the coefficients d_n, d_ϕ, D_{nn}, $D_{\phi\phi}$, and $D_{n\phi}$ around mean values $\langle n\rangle(t)$ and $\langle\phi\rangle(t)$, we have the same equations as (5.18), (5.19), and (5.20), except now $\delta n=n-n_0$ is changed to $\delta n=n-\langle n\rangle(t)$ and $\delta\phi=\phi-\phi_0$ to $\delta\phi=\phi-\langle\phi\rangle(t)$.

First, we show in Fig. 19 the intensity as a function of time for different initial conditions. Three trajectories starting at $n(0)=0.1$, $n(0)=2$, and $n(0)=4$, respectively, lead to the same stationary values. Obviously they have different transient behavior.

As discussed earlier, there is no squeezing of phase noise in the steady state. The reason is the vanishing of the pumping statistics term in the phase diffusion coefficient $D_{\phi\phi}$ in the steady state. In the transient regime, we can have a nonzero pumping statistics term.

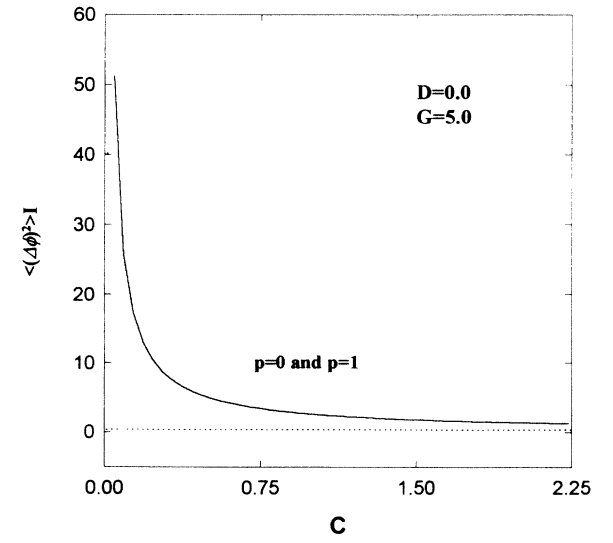

FIG. 16. Phase noise as a function of the amplitude of atomic coherence C. The parameters are the same as in Fig. 15. The dotted line corresponds to the vacuum noise level.

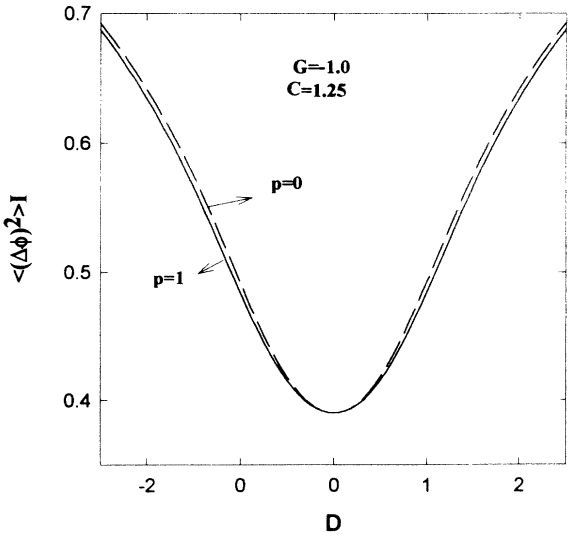

FIG. 18. Phase noise as a function of detuning D. The parameters are the same as in Fig. 17.

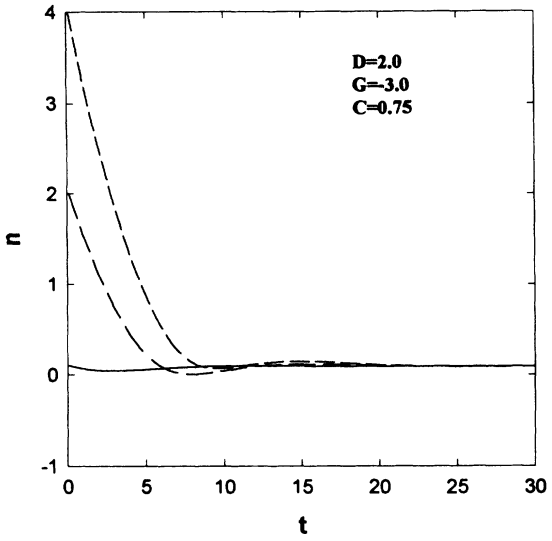

FIG. 19. Typical intensity transients for different initial conditions $n(0)=4$, $n(0)=2$, and $n(0)=0.1$, respectively. The parameters are $A=2.5$, $D=2.0$, $G=-3.0$, and $C=0.75$.

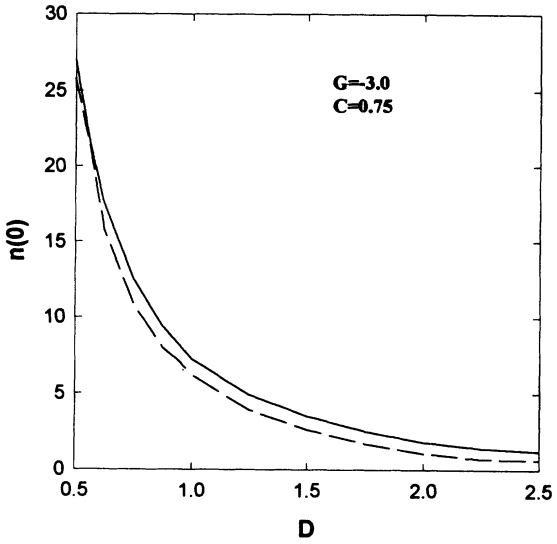

FIG. 21. Squeezing boundaries for a given detuning. Transient phase noise squeezing occurs if the initial intensity is between the dashed line and solid line. Parameters are same as in Fig. 19.

This nonzero pumping statistics term leads to the transient squeezing of phase noise. This can easily be seen from Eq. (5.9). For nonzero detuning D and sufficiently large initial intensity $n(0)$, the term D^2 becomes the leading one in the phase diffusion coefficient. Under these conditions, the value of $D_{\phi\phi}$ is negative and, thus, the squeezing of phase noise occurs. We show this transient phase noise $\langle(\Delta\phi)^2\rangle I$ in Fig. 20 with $D=2$, $A=2.5$, $G=-3$, $C=0.75$ for three initial intensities, $n(0)=0.1$, $n(0)=2$, and $n(0)=4$, respectively. The curve starting at $n(0)=0.1$ is larger than the squeezing limit 0.25, everywhere. A transient squeezing of phase noise occurs for the curve with $n(0)=2$. The inverted peak corresponds to the minimum of the curve depicted in Fig. 19. But there is an unphysical transient behavior for the curve with $n(0)=4$. This means that there are some limitations on the permissible initial intensities and other parameters where we are allowed to employ a linearized treatment. Using $\langle(\Delta I)^2\rangle\langle(\Delta\phi)^2\rangle=0.25$, we can find the conditions under which the uncertainty principle is satisfied. The results are displayed in Fig. 21. Other parameters are the same as in Fig. 20. The region under the solid line is compatible with the uncertainty principle. Of

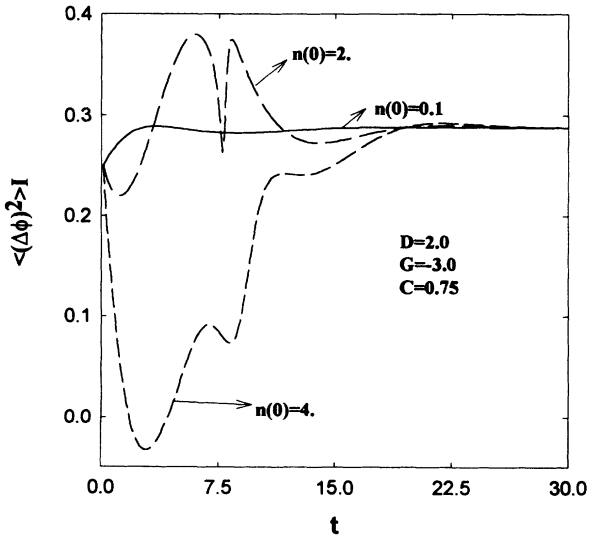

FIG. 20. Typical phase noise transients for different initial conditions $n(0)=4$, $n(0)=2$, and $n(0)=0.1$, respectively, with $p=1$. Parameters are the same as in Fig. 19.

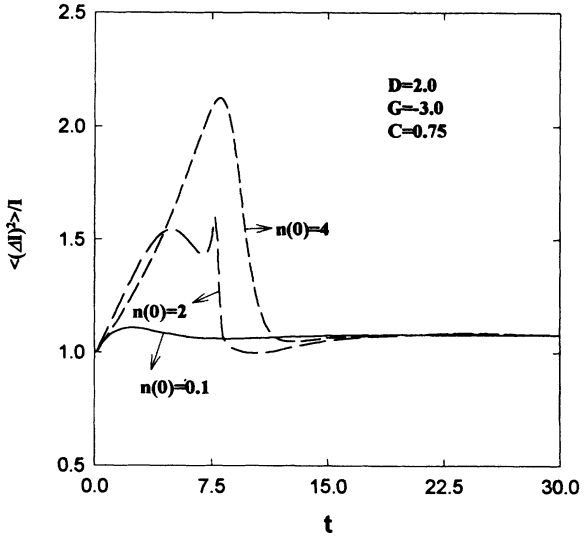

FIG. 22. Typical intensity noise transients for different initial conditions $n(0)=4$, $n(0)=2$, and $n(0)=0.1$, respectively, with $p=1$. Parameters are the same as in Fig. 19.

course, this does not mean that the uncertainty principle is violated outside this region. It simply means that our quasilinearized treatment breaks down for initial conditions that are too far off the stationary solutions. Above the dashed line squeezing of the phase noise occurs. We plot the intensity noise as a function of time in Fig. 22. The parameters are the same as in Fig. 20.

VI. CONCLUSION

We have analyzed the influence of the injected atomic coherence on laser operation. The numerical results for the intensity and phase of the laser have been obtained from the semiclassical equations of motion. We have discussed the steady-state laser operation first. It has been shown that lasing without population inversion occurs in the system. We have also found that, in the usual laser regime, i.e., above threshold, the plot of intensity vs amplitude of atomic coherence, $n_0(C)$, becomes S-shaped (Figs. 2–4), similarly to optical bistability. With the help of linear stability analysis we have shown that both below and above threshold the $n_0(C)$ curve contains unstable parts. The size of the unstable region increases with increasing cavity-field detuning. In the unstable region both the intensity and phase exhibit periodic oscillations. We gave an analytic expression for the oscillation frequency.

In the stable region, the operating frequency of the laser is locked to the atomic frequency. This requires that $C > C_c$ where, in turn, the critical coherence is a function of the detuning D and gain G in such a way that with increasing detuning the instability region also increases. In the unstable region, in addition to the oscillatory behavior of the intensity and phase, there is also a shift in the operating frequency of the laser. This shift is such that our expression reduces to the frequency pulling expression of an incoherently pumped laser when the amplitude of the injected coherence is zero and rises monotonically with increasing C to match the atomic frequency at the critical point. We can, thus, interpret the unstable region as a competition between the atomic frequency and the pulled frequency of a detuned laser. The coherence in this region is not sufficient to maintain stable locking to the atomic frequency but, via the driving terms in the nonlinear equations of motion, it makes the laser feel its presence in the dynamics and leads to the constant interplay between these two frequencies. A study of the trajectories of the laser reveals that in this case there is a stable limit cycle in the phase plane of the quadratures.

We have investigated the influence of the pumping statistics on the laser with injected atomic coherence. We have found that with random pumping statistics ($p=0$) there is quantum noise reduction for both intensity and phase, but there is no squeezing for any of them, because the diffusion coefficients D_{II} and $D_{\phi\phi}$, although reduced by ρ_{ab}, remain always larger than zero ($D_{II} \geq 0$ and $D_{\phi\phi} > 0$). In the present paper, we have focused our attention on the regular pumping statistics ($p=1$). In steady state the regular distribution leads to the squeezing of the intensity noise. For short times the phase noise is squeezed (transient squeezing) and the solutions crucially depend on the initial intensity.

ACKNOWLEDGMENT

We gratefully acknowledge the support of the Office of Naval Research (Grant No. N00014-92-J-1233) and a PSC-CUNY Research Grant.

[1] M. O. Scully and W. E. Lamb, Jr., Phys. Rev. **159**, 208 (1967); H. Haken, *Laser Theory,* edited by L. Genzel, Handbuch der Physik Vol. 25 (Springer, Berlin, 1970), Part 2c; W. H. Louisell, *Quantum Statistical Theory of Radiation* (Wiley, New York, 1973).

[2] M. B. Spencer and W. E. Lamb, Jr., Phys. Rev. A **5**, 884 (1972); W. W. Chow, M. O. Scully, and E. W. van Stryland, Opt. Commun. **15**, 258 (1975).

[3] H. Zeglache and V. Zehnlé, Phys. Rev. A **46**, 6015 (1992).

[4] M. O. Scully, Phys. Rev. Lett. **55**, 2802 (1985); M. O. Scully, K. Wódkiewicz, M. S. Zubairy, J. Bergou, N. Lu, and J. Meyer ter Vehn, *ibid.* **60**, 1832 (1988).

[5] N. Lu and J. Bergou, Phys. Rev. A **40**, 237 (1989).

[6] T. Carty and M. Sargent III, Phys. Rev. A **42**, 1544 (1990).

[7] C. Benkert, M. O. Scully, and M. Orszag, Phys. Rev. A **42**, 1487 (1990).

[8] S. E. Harris, Phys. Rev. Lett. **62**, 1033 (1989); M. O. Scully, S.-Y. Zhu, and A. Gavrielides, *ibid.* **62**, 2813 (1989).

[9] J. A. Bergou and P. Bogar, Phys. Rev. A **43**, 4889 (1991).

[10] M. Sargent III, M. O. Scully, and W. E. Lamb, Jr., *Laser Physics* (Addison-Wesley, Reading, MA, 1974).

[11] J. A. Bergou, L. Davidovich, M. Orszag, C. Benkert, M. Hillery, and M. O. Scully, Phys. Rev. A **40**, 5073 (1989).

[12] C. Benkert, M. O. Scully, J. A. Bergou, L. Davidovich, M. Hillery, and M. Orszag, Phys. Rev. A **41**, 2756 (1990).

[13] M. A. M. Marte and D. F. Walls, Phys. Rev. A **37**, 1235 (1987); M. A. M. Marte, H. Ritsch, and D. F. Walls, Phys. Rev. Lett. **61**, 1093 (1988); Phys. Rev. A **38**, 3577 (1988); M. C. Teich and B. E. A. Saleh, J. Opt. Soc. Am. B **2**, 275 (1985); S. Machida, Y. Yamamoto, and Y. Itaya, Phys. Rev. Lett. **58**, 1000 (1987); S. Machida and Y. Yamamoto, *ibid.* **60**, 792 (1988); Y. M. Golubev and I V. Sokolov, Zh. Eksp. Teor. Fiz. **84**, 408 (1984) [Sov. Phys. JETP **60**, 234 (1984)]; Y. Yamamoto, S. Machida, and O. Nilsson, Phys. Rev. A **34**, 4025 (1986); **35**, 5114 (1987); M. A. M. Marte and P. Zoller, *ibid.* **40**, 5774 (1989); T. A. B. Kennedy and D. F. Walls, *ibid.* **40**, 6366 (1989); F. Haake, S. M. Tan, and D. F. Walls, *ibid.* **40**, 7121 (1989); **41**, 2808 (1990).

[14] J. A. Bergou, M. Orszag, and M. O. Scully, Phys. Rev. A **38**, 754 (1988); **38**, 763 (1988); **38**, 768 (1988).

[15] M. O. Scully and M. S. Zubairy, Phys. Rev. A **35**, 752 (1987); W. Schleich and M. O. Scully, *ibid.* **37**, 1261 (1988).

[16] J. Gea-Banacloche, Phys. Rev. Lett. **59**, 543 (1987); N. Lu and J. A. Bergou, Phys. Rev. A **40**, 250 (1989); J. A. Bergou, N. Lu, and M. O. Scully, Opt. Commun. **73**, 57

(1989).
[17] C. Benkert, M. O. Scully, J. Bergou, and M. Orszag, Phys. Rev. A **41**, 4069 (1990); C. Benkert and M. O. Scully, *ibid.* **42**, 2817 (1990).
[18] G. S. Agarwal, J. Bergou, C. Benkert, and M. O. Scully, Phys Rev. A **43**(RC), 6451 (1991).
[19] A. Hourri, MS thesis, Hunter College of CUNY, 1992 (unpublished).
[20] J. Bergou, M. Orszag, M. O. Scully, and K. Wodkiewicz, Phys. Rev. A **39**, 5136 (1989).
[21] J. Bergou and M. Hillery, Phys. Rev. A **49**, 1214 (1994).